Metastability in the ferrimagnetic–antiferromagnetic phase transition in Co substituted Mn_2Sb

2008 J. Phys.: Condens. Matter 20 022204

(http://iopscience.iop.org/0953-8984/20/2/022204)

IOP FTC
IOP PUBLISHING JOURNAL OF PHYSICS: CONDENSED MATTER
J. Phys.: Condens. Matter **20** (2008) 022204 (7pp) doi:10.1088/0953-8984/20/02/022204

FAST TRACK COMMUNICATION

Metastability in the ferrimagnetic–antiferromagnetic phase transition in Co substituted Mn_2Sb

Pallavi Kushwaha, R Rawat and P Chaddah

UGC-DAE Consortium for Scientific Research, University Campus, Khandwa Road, Indore-452001, India

E-mail: rrawat@csr.ernet.in

Received 20 November 2007
Published 13 December 2007
Online at stacks.iop.org/JPhysCM/20/022204

Abstract

A detailed investigation of the first-order ferrimagnetic (FRI) to antiferromagnetic (AFM) transition in $Mn_{1.85}Co_{0.15}Sb$ is carried out. These measurements demonstrate anomalous thermomagnetic irreversibility and a glass-like frozen FRI phase at low temperatures. The irreversibility arising between the supercooling and superheating spinodals is distinguished in an ingenious way from the irreversibility arising due to kinetic arrest. Field annealing measurements show a re-entrant FRI–AFM–FRI transition with increasing temperature. In this system the kinetic arrest band and supercooling band are also shown to be anticorrelated (i.e. the regions which are kinetically arrested at higher temperature have lower supercooling temperature and vice versa), which has been a universal feature of the AFM/ferromagnetic transition so far.

(Some figures in this article are in colour only in the electronic version)

1. Introduction

The compound Mn_2Sb crystallizes in Cu_2Sb type tetragonal structure and orders ferrimagnetically (FRI) below $T_C \approx 550$ K [1, 2]. There are two crystallographically non-equivalent sites for Mn atoms, Mn(I) and Mn(II), which are tetrahedrally and octahedrally surrounded by Sb atoms. The magnetic structure of this compound consists of Mn(I)–Mn(II)–Mn(I) triple layers where magnetic moments of Mn(I) (2.1 μ_B) and Mn(II) (3.9 μ_B) are aligned antiparallel to each other. These triple layers align parallel to each other resulting in the ferrimagnetic state. The substitution of various elements (V, Cr, Co, Cu and Zn) for Mn as well as (As, Ge, Sn) for Sb results in the appearance of a first-order FRI to antiferromagnetic (AFM) transition with decreasing temperature [3–9]. In the AFM state Mn(I)–Mn(II)–Mn(I) triple layers align antiparallel to each other [10]. The FRI to AFM transition at T_N is accompanied with large change in unit cell volume, resistivity, magnetization etc [8, 9, 11–13]. Below the FRI to AFM transition temperature T_N, application of magnetic field induces a first-order AFM to FRI transition which give rise to large magnetoresistance, magnetostriction etc [9, 11, 12]. There has been considerable interest in these compounds due to these effects of magnetic field along with the tunability of the transition temperature up to and above room temperature.

However, in spite of various studies on the doped Mn_2Sb there are very few studies on the low temperature behavior of these systems. There are a few reports which do indicate anomalous low temperature behavior in these systems. Zhang *et al* (for $Mn_2Sb_{0.95}Sn_{0.05}$) [12] and Bartashevich *et al* (for $Mn_{1.80}Co_{0.20}Sb$ under 10 kbar pressure) [8] have observed a virgin curve lying outside the envelope curve in their magnetization versus magnetic field measurements at low temperatures. The H–T phase diagram based on high magnetic field studies of Co substituted Mn_2Sb shows a broadening of the hysteretic region with decreasing temperature and a shallow maxima around 40 K for lower critical field (field required for the FRI to AFM transition) [8]. Similar non-monotonic behavior for lower

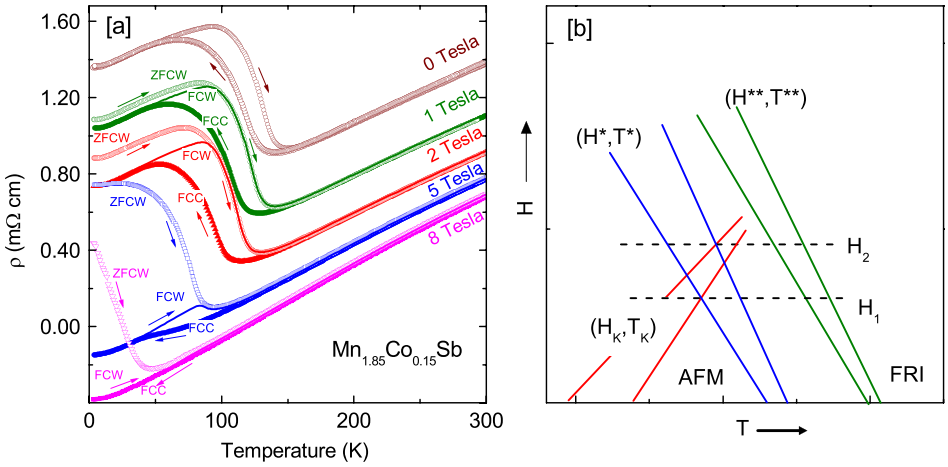

Figure 1. (a) Resistivity as a function of temperature in the presence of various constant magnetic fields. The measurements were made in the presence of a labeled magnetic field where ZFCW is measured during warming after zero-field cooling, FCC during cooling in a field and FCW during warming after field cooling in the same field. The scale on the y-axis is for the 0 T curve and the other curves are shifted downward for the sake of clarity. The resistivity values at 300 K are independent of H on this scale. (b) Schematic of the kinetic arrest (H_K, T_K), supercooling (H^*, T^*) and superheating (H^{**}, T^{**}) bands in H–T space adapted from Banerjee *et al* [19]. The coexisting phases will be observed at the lowest temperature only if the cooling or annealing field H lies between H_1 and H_2. See the text for details.

critical field (ferromagnetic to AFM transition) has been observed at low temperature for $Nd_{0.5}Sr_{0.5}MnO_3$ [14–16] which shows an anomalous thermomagnetic irreversibility. Such anomalous behavior in the first-order transition at low temperature is of current interest for its implications in the physics of manganites and glasses [17–19].

In the present study, we carry out detailed investigation of the first-order transition in $Mn_{1.85}Co_{0.15}Sb$ at low temperatures. This study shows that the critically slow dynamics of the phase transition at low temperature results in glass-like kinetic arrest [17–19] of the high temperature FRI phase. The observed irreversibility at low temperatures (due to kinetic arrest) and irreversibility around the transition temperature (due to supercooling and superheating effects) are distinguished. By following novel paths in the H–T space one can observe a glass-like FRI phase at low temperature and the system shows re-entrant FRI to AFM to FRI transitions with increasing temperature. These measurements also show tunability of coexisting FRI and AFM phase fractions and reveal an anticorrelation between supercooling and kinetic arrest bands. This system is the first FRI system which can be placed alongside intermetallic systems like doped $CeFe_2$ [17, 20], Gd_5Ge_4 [21], Nd_7Rh_3 [22] where such an arrest of kinetics was observed.

2. Experimental details

The compound $Mn_{2-x}Co_xSb$ with $x = 0.15$ is prepared by arc melting of the constituent elements (purity better than 99.99%, LIECO Industries, USA) under high purity Argon atmosphere. Powder x-ray diffraction of the prepared compound shows that the compound crystallizes in Cu_2Sb type tetragonal structure and there are no impurity peaks. The resistivity measurements are performed by the standard four-probe technique using a commercial cryostat (Oxford Instruments Inc., UK) in the temperature range 3–300 K and up to 8 T magnetic fields. For in-field measurements magnetic field is applied parallel to the current direction.

3. Results and discussion

Figure 1(a) shows the temperature dependence of the resistivity in the presence of various constant magnetic fields for $Mn_{1.85}Co_{0.15}Sb$. A sharp rise in the zero-field resistivity with decreasing temperature indicates the transition from the low resistance FRI to the high resistance AFM phase. It must be noted here that both phases are metallic in nature and the negative resistivity slope in the transition region is due to the increase in the AFM phase fraction (high resistivity) with lowering temperature. During warming, the transition occurs at higher temperature resulting in a thermal hysteresis across the transition. This thermal hysteresis indicates the first-order nature of the transition. The transition temperature which is taken as the inflection point of the resistivity curve is found to be ≈118 K during cooling and ≈132 K during the warming cycle and these are in good agreement with reported zero-field transition temperatures for this composition [8, 11]. Besides this, it is also observed that the room temperature resistivity increases (≈1%) on the initial thermal cycling through the transition. It is well known that in this compound the AFM to FRI transition is accompanied with large volume change which can result in microcracks and hence increased resistivity during the transition [8]. We have taken care of this during the interpretation of our results and such effects are minimized by repeated thermal cycling of the sample. As can be seen from figure 1 the transition width is broad (≈60 K) during both cooling and heating. The broadening of the first-order transition can arise due to chemical inhomogeneity or disorder inherent in substitutional alloys. In a disorder-free sample the first-order transition will occur at a sharply defined (H_C, T_C) line. Due to disorder, different regions having length scales of the order of the correlation length can

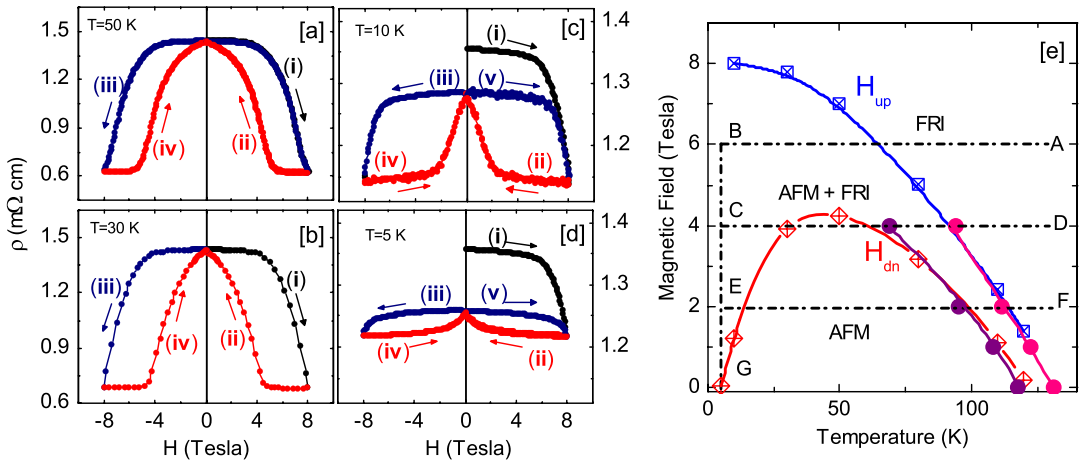

Figure 2. ((a)–(d)) Isothermal R versus H for $Mn_{1.85}Co_{0.15}Sb$ at various temperatures. The open R–H loop and the virgin curve lying outside the envelope curve are apparent at low temperature. (e) H–T phase diagram for $Mn_{1.85}Co_{0.15}Sb$ obtained from R–H (crossed squares) and R–T measurements (solid circles). See the text for details.

have different transition temperatures, and this results in the transition line broadening into a band [23–25]. Supercooling (H^*, T^*) and superheating (H^{**}, T^{**}) spinodals will also form a band for such a sample [23]. Though broad transitions are undesirable for many applications, in the present study they will be useful for studying phase coexistence and correlation between supercooling and kinetic arrest (H_K, T_K) bands. The kinetic arrest band in H–T space defines a set of lines below which the dynamics of the transition is slow and inhibited on experimental timescales. This is illustrated in figure 1(b), which shows a schematic diagram of kinetic arrest (H_K, T_K) band and supercooling (H^*, T^*)/superheating (H^{**}, T^{**}) bands adapted from Banerjee *et al* [19]. Here H_1 and H_2 are the lower and upper limits of the magnetic field in which the (H_K, T_K) band overlaps with the (H^*, T^*) band. The interplay between the kinetic arrest and supercooling takes place when field cooling is done with fields lying between H_1 and H_2 resulting in a coexisting arrested (FRI) and a stable (AFM) phase at low temperature [19]. If the bandwidths are narrow then the field window ($H_2 - H_1$) will decrease and become zero in the limit of zero bandwidth so there will be no phase coexistence; the system will be either in a completely AFM state or in a completely arrested FRI state.

The FRI to AFM transition is suppressed with the application of magnetic field which can be seen from the resistivity behavior in the presence of various magnetic fields in figure 1(a). This also highlights the history dependence of the resistivity behavior. The resistivity behavior below T_N in figure 1(a) shows that resistivity measured during warming after zero-field cooling (ZFCW) is higher than that measured during cooling (FCC) and subsequent warming (FCW) under the same field. Here it is worth mentioning that the higher resistivity for the ZFCW curve compared to the FCC/FCW (i.e. FC) curve is an intrinsic property of the sample. It is not due to microcracks caused by thermal cycling since the ZFCW curve which has higher resistivity was measured before the FC curve. With increasing magnetic field the difference between ZFCW and FC curves increases. For 8 T field there is no signature of an FRI to AFM transition for FC measurement. Such thermomagnetic irreversibility for resistivity in ZFCW and FC curves has been observed in many other systems across the first-order transition—like in transition metal doped $CeFe_2$ [17, 20], $Nd_{0.5}Sr_{0.5}MnO_3$ [16] etc. In these systems it has been attributed to coexisting phases whose ratio depends on the path traversed in the H–T space.

Such path dependence is also observed in the isothermal magnetoresistance (R–H) shown in figures 2(a)–(d). For these measurements samples were cooled under zero field from well above T_N to the measurement temperature. With the application of magnetic field, a field-induced transition from the AFM to the FRI phase is observed as a sharp decrease in resistivity. The reverse transformation occurs at a lower field value resulting in a hysteretic field dependence of resistivity. At 50 and 30 K, the resistivity reaches its ZFC value at 0 T which indicates the complete reverse transformation from the FRI to the AFM phase. Further cycling for these field values in the negative direction results in a mirror image of the R–H curve obtained for the positive field cycle. At lower temperatures anomalous behavior was observed, as shown for 10 and 5 K in figures 2(c) and (d). With increasing magnetic field a partial phase transformation from the AFM to the FRI phase is observed as 8 T field is not sufficient for completing the transformation. With decreasing magnetic field the reverse transformation starts at lower field with decreasing temperature and this transformation does not complete even when the magnetic field is reduced to zero. Therefore the zero-field resistivities before and after the application of the magnetic field show a large difference and this anomalous difference increases with decreasing temperature. For further cycling of the magnetic field an envelope curve is obtained with much smaller variation of the resistivity compared to the virgin curve. Also the virgin curve lies outside the envelope curve. Earlier magnetization versus magnetic field measurements on $Mn_{1.8}Co_{0.2}Sb$ also showed the virgin curve lying outside the envelope curve at 4.2 K when measured under 10 kbar pressure [8]. In the case of magnetization measurements, opening of a hysteresis loop at zero field is not observed as

the magnetization goes to zero for the FRI state also. However the magnetic state at zero field is clearly demonstrated in R–H measurements in the present study, where distinctly lower resistivity at zero field is observed after field cycling.

The H–T diagram obtained from R–T and R–H measurements is shown in figure 2(e). The transition temperature and field are taken as the minima of the first-order derivatives of these curves, respectively. This phase diagram is consistent with earlier reports on Co doped Mn_2Sb [8]. Both FRI and AFM phases coexist between H_{up} and H_{dn} and completely homogeneous FRI (AFM) phase is obtained above H_{up} (below H_{dn}). Such broadening of the hysteretic region has been observed in many manganite systems [14, 15], transition metal doped FeRh [26] and is generally associated with a first-order transition at low temperatures. Besides broadening of the hysteresis region this figure also shows the non-monotonic variation of the lower critical field required for the FRI to AFM transition. It has been shown in the case of $Nd_{0.5}Sr_{0.5}MnO_3$ [16] that such non-monotonic behavior is anomalous and cannot be explained in terms of a conventional first-order transition. Such behavior arises due to critically slow dynamics of the first-order transition at low temperature and the high temperature phase remains arrested at low temperatures. Therefore anomalous behavior in the present case will also be discussed in terms of kinetic arrest and the decreasing lower critical field with decreasing temperature is a reflection of the kinetic arrest band for this compound. The anomalous thermomagnetic irreversibility then can be explained as due to an arrested FRI phase at low temperatures.

It has been argued that field-induced first-order magnetic transitions provide an experimentally versatile platform for studying glass-like kinetic arrest [23]. Since the transformation is H induced, the transition temperature (T_N) obtained under constant H cooling/heating must vary with H. For some systems this T_N is low enough for the kinetic arrest temperature T_K to interfere and hinder the transition. Since T_N depends on H, one can vary H from a situation where $T_K < T^*$ to one where $T_K > T^*$ [28]. In the former case rapid cooling is essential for glass formation, like in Metglasses. In the latter case a comparatively slow cooling can result in a glass, like in the glass former O-terphenyl. Field-induced first-order magnetic transitions provide an experimental platform where the variation of H allows us to study very different glass-formation behaviors in the same system; traversing novel paths in (H, T) space provides interesting new phenomena [16–21, 28, 27, 29]. We now show that H-induced first-order magnetic transitions also provide a fertile platform for studying supercooled/superheated metastable states.

As has been argued earlier [19], the slope of the $T_N(H)$ line is dictated by the magnetic order in the low T zero-field state and is negative for the present sample. This is schematically shown in figure 3(a) along with the supercooling and superheating spinodals $T^*(H)$ and $T^{**}(H)$, respectively. We now consider that we reach (in zero field) a certain temperature T_0 (point Q) lying between $T^*(0)$ and $T^{**}(0)$. If we have reached T_0 by cooling (say point P to Q), then

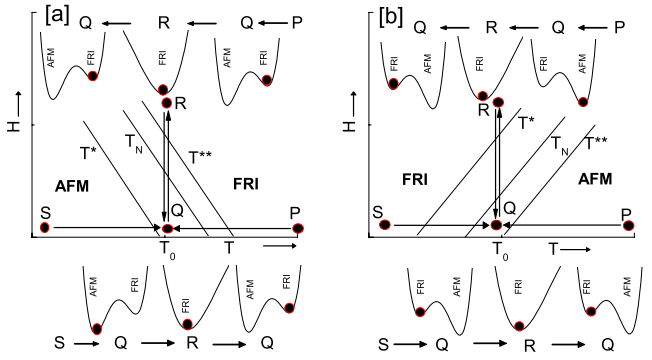

Figure 3. Transformations in the supercooling or superheating regime for different paths are demonstrated along with a corresponding schematic of the free energy diagram. The state in which the system exists is indicated by the filled circle. Note that in the case (a) an open hysteresis loop will be seen only if T_0 is reached on heating, and in case (b) only if T_0 is reached on cooling. In these cases the virgin state and remnant states are different; and the remnant state is independent of whether T_0 is reached by heating or cooling.

the initial state is a metastable supercooled FRI phase. A subsequent isothermal cycling of the field at T_0 (Q to R to Q) takes the sample from a metastable FRI state to a stable FRI state and back to a metastable FRI state, respectively. If however, we reach T_0 by heating (path S to Q), then the starting $H = 0$ state is a stable AFM state. As H is raised, it transforms to stable FRI at $H^{**}(T_0)$ but returns to metastable FRI at $H = 0$. The initial and final states at $H = 0$ (at point Q) are thus different and we will observe an open loop in R versus H. This open loop will not be observed when T_0 is reduced to below T^* or raised above T^{**}.

If the low T zero-field state is FRI, as shown in the schematic in figure 3(b), then the anomalous open loop will be observed on reaching T_0 by cooling in zero field from P to Q (and not on heating, i.e. S to Q) when T_0 will be between $T^*(0)$ and $T^{**}(0)$. This experimental check for an open loop on cooling versus heating thus cross-checks the low T zero-H state. The open loop will not be observed as T_0 is lowered below T^* in this case also. This latter feature contrasts with the case of kinetic arrest where the open loop becomes more prominent as T_0 is lowered [14, 16, 17].

Figure 4 shows the R–H curve for temperatures 60, 120, 130 and 160 K. For each of these measurements the sample was cooled down to 5 K and then warmed to the measurement temperature under zero-field conditions before taking measurements. Since 60 K and 160 K are below $T^*(0)$ and above $T^{**}(0)$ respectively, the initial ZFCW states at $H = 0$ are stable states as also are the remnant states. At 60 K, we observe a field-induced transition but not at 160 K. At 120 and 130 K, the initial ZFCW states are AFM (with higher resistance) but the remnant states are FRI (with lower resistance). This is consistent with the schematic shown in figure 3(a). Because of disorder broadening, the initial state will also have a stable FRI phase coexisting with the AFM phase. With the application of a magnetic field the AFM phase (both stable and metastable) will transform to an FRI phase completely on crossing the H^{**} band. However

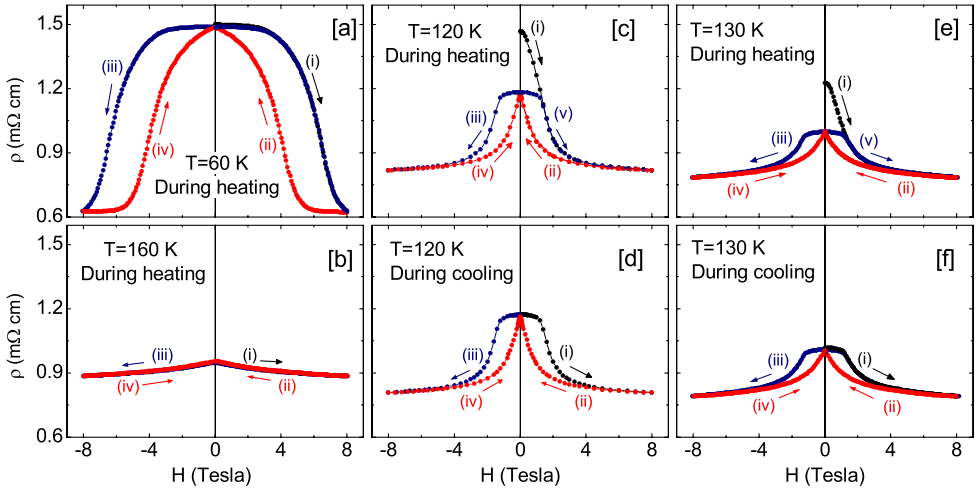

Figure 4. Magnetic field dependence of the resistivity (R–H) at $T_0 = 60$, 160, 120 and 130 K with T_0 being reached by heating from 5 K. The different zero-field resistivities before and after the application of the magnetic field during heating at 120 K (c) and 130 K (e) are highlighted, whereas no such difference is observed when $T_0 = 120$ K (d) and 130 K (f) are reached by cooling, consistent with figure 3(a).

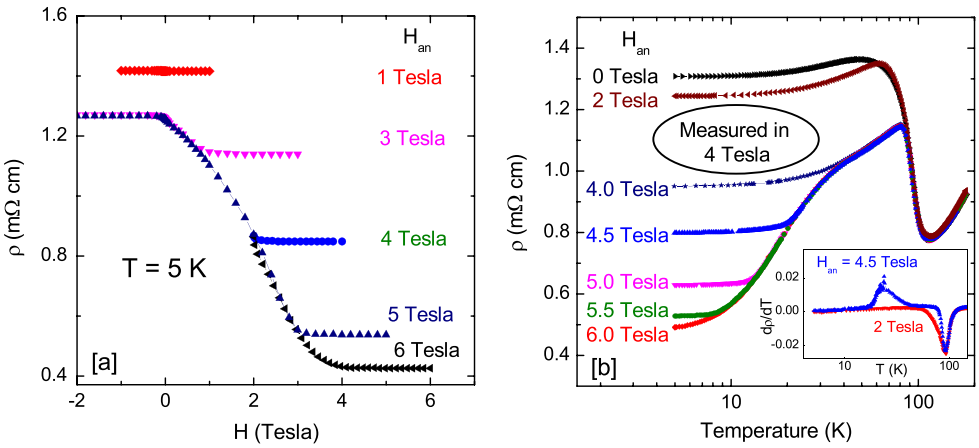

Figure 5. (a) De-arrest of the FRI phase is shown with reducing magnetic field at 5 K in the R–H measurement for samples cooled under various annealing fields H_{an}. The merging of R–H curves with reducing magnetic field suggests anticorrelation [23]. See the text for details. (b) Re-entrant phase transition from the FRI to the AFM to the FRI state is shown in the temperature dependence of the resistivity in the field of 4 T during warming. Samples were cooled under the annealing field H_{an}. The inset highlights that two transitions are seen only when the cooling (or annealing) field H_{an} is larger than the measuring field which is consistent with the low T, low H ground state being AFM [19]. The curve for higher H_{an} merges at lower temperature showing anticorrelation between the supercooling and kinetic arrest bands [23]. See the text for details.

with reducing magnetic field it will not transform back to the initial state and reverse transformation will take place only for those regions of sample for which T^* line is crossed on reducing the magnetic field. Since the state of the system is different before and after the application of magnetic field, we observe an open hysteresis loop at these temperatures. Further field cycling produces a symmetric envelope curve. This envelope curve will be similar to an R–H curve at the same temperature when reached during cooling. This is shown in figures 4(d) and (f) for 120 K and 130 K respectively, where R–H measurements were performed at these temperatures after cooling the sample from room temperature under zero-field conditions. The R–H curve during cooling shows no difference between the virgin curve and the envelope curve at these temperatures and these R–H curves overlap with the respective R–H envelope curves obtained during heating.

We have shown that the behavior of the metastable supercooled state is distinct from the metastable kinetically arrested state at low temperature. This brings out very clearly the difference between supercooling and glass-like kinetic arrest. Now we study the transformation of the kinetically arrested FRI state to a stable AFM state. For this we controlled the arrested FRI fraction by field annealing at various fields and its transformation is studied as a function of magnetic field and temperature. For these measurements the sample is cooled from room temperature to 5 K under an applied magnetic field H_{an}. Then at 5 K, the magnetic field is reduced isothermally to 0 T and resistivity is measured as a function of magnetic field which is shown in figure 5(a). The lower

resistivity at higher H_{an} indicates a larger fraction of FRI phase, and brings out the tunability of phase fractions at 5 K. The resistivity dependence on the annealing field H_{an} is evident from figure 2(e) which shows that along path A to B one obtains a higher FRI phase fraction as compared to path D to C, and this arrested FRI phase will transform back to an AFM phase on reducing the magnetic field only after crossing the kinetic arrest band. As can be seen in figure 5(a), the R–H curve remains constant initially and then shows a rapid increase with decreasing magnetic field indicating the de-arrest of the FRI phase into an AFM phase. The R–H curves for H_{an} from 3 to 8 T merge on reducing the magnetic field whereas the 1 T curve remains at higher values. In fact the resistivity for 1 T annealing field remains almost constant and is distinctly higher compared to that for higher annealing fields. This implies that H_1 (figure 1(b)) for this sample could be lying above 1 T magnetic field. These trends are similar to those expected for anticorrelated supercooling and kinetic arrest bands, i.e. regions which have lower supercooling temperature are arrested at higher temperature [27, 23, 29].

The kinetically arrested FRI phase can show de-arrest with increasing temperature also. In such cases the FRI phase transforms to an AFM phase with increase temperature. To demonstrate this, a sample is cooled in the presence of H_{an} to 5 K and then the magnetic field is changed to 4 T isothermally. Then R versus T measurements are carried out during heating in the presence of 4 T; the results are shown in figure 5(b). A re-entrant FRI to AFM to FRI transition is clearly visible for all the FCW curves for which H_{an} is larger than the measurement field of 4 T, whereas only one AFM to FRI transition is observed for $H_{an} \leqslant 4$ T. This is evident from figure 2(e), in which path ABCD corresponds to $H_{an} \geqslant 4$ T and path FECD corresponds to $H_{an} \leqslant 4$ T. Across path ABC we obtain an arrested FRI phase which shows de-arrest to an AFM state on crossing the kinetic arrest band which then transforms back to an FRI phase after crossing the (H^{**}, T^{**}) band. This is brought out very clearly in the inset where we plot the temperature derivative of the resistivity $(\mathrm{d}R/\mathrm{d}T)$ for $H_{an} = 2$ and 4.5 T. The fact that two transitions are seen only when the annealing field H_{an} is larger than the measuring field is consistent with the low temperature, low field ground state being AFM [19]. The AFM to FRI transition is independent of the annealing field H_{an} whereas the FRI to AFM transition depends on H_{an}. For lower H_{an}, the FRI to AFM transition starts at higher temperature compared to that for higher H_{an}. It is evident from this figure that the resistivity for $H_{an} \leqslant 5.5$ T remains constant initially and then shows an upturn with increasing temperature. The temperature where the resistivity shows an upturn is higher for lower H_{an}. Also the curves for higher H_{an} merge at lower temperature and all the curves for $H_{an} \geqslant 4.5$ T merge before merging to the FC 4 T curve during warming. All these features are similar to those seen in earlier studies on very different materials and the de-arrest as a function of temperature once again is similar to that expected for anticorrelated supercooling and kinetic arrest bands [27, 23, 29].

4. Conclusions

To conclude, a detailed investigation of the first-order FRI to AFM transition is carried out at low temperatures. These studies reveal anomalous thermomagnetic irreversibility along with non-monotonic variation of the lower critical field at low temperatures. These anomalies are interpreted in terms of kinetic arrest of the FRI phase due to critically slow dynamics of transformation on the measurement timescale. The irreversibilities due to kinetic arrest are distinguished from those arising due to metastability in the supercooling or superheating regime. Below the transition temperature, FRI and AFM phases can coexist over a wide temperature and magnetic field range, and tunability of these phases is demonstrated. The measurements also show anticorrelation between the kinetic arrest band and supercooling band. Similar anticorrelation was observed earlier for the AFM to FM transition in intermetallic and manganite systems. This study extends this universality to the FRI to AFM transition.

Acknowledgment

We acknowledge Dr Alok Banerjee for valuable discussion and suggestions.

References

[1] Beckman O and Lundgren L 1991 *Handbook of Magnetic Materials* vol 6, ed K H J Buschow (Amsterdam: Elsevier) chapter 3, p 181
[2] Wilkinson M K, Gingrich N S and Shull C G 1957 *J. Phys. Chem. Solids* **2** 289
[3] Kanomata T and Ido H 1984 *J. Appl. Phys.* **55** 2039
[4] Swoboda T J, Cloud W H, Bither T A, Sadler M S and Jarrett H S 1960 *Phys. Rev. Lett.* **4** 509
[5] Bither T A, Walter P H L, Cloud W H, Swoboda T J and Bierstedt P E 1962 *J. Appl. Phys.* **33** (Suppl.) 1346
[6] Darnell F J, Cloud W H and Jarrett H S 1963 *Phys. Rev.* **130** 647
[7] Wijngaard J H, Haas C and de Groot R A 1992 *Phys. Rev.* B **45** 5395
[8] Bartashevich M I, Goto T, Tomita T, Baranov N V, Zemlyanski S V, Hilscher G and Michor H 2002 *Physica* B **318** 198
[9] Zhang Y Q and Zhang Z D 2003 *Phys. Rev.* B **67** 132405
[10] Austin A E, Adelson E and Cloud W H 1963 *Phys. Rev.* **131** 1511
[11] Bartashevich M I, Goto T, Baranov N V and Gaviko V S 2004 *Physica* B **351** 71
[12] Zhang Y Q, Zhang Z D and Aarts J 2004 *Phys. Rev.* B **70** 132407
Zhang Y Q, Zhang Z D and Aarts J 2005 *Phys. Rev.* B **71** 229902(E)
[13] Bierstedt P E 1963 *Phys. Rev.* B **132** 669
[14] Kuwahara H, Tomioka Y, Asamitsu A, Moritomo Y and Tokura Y 1995 *Science* **270** 961
[15] Tokura Y 2006 *Rep. Prog. Phys.* **69** 797
[16] Rawat R, Mukherjee K, Kumar K, Banerjee A and Chaddah P 2007 *J. Phys.: Condens. Matter* **19** 256211
[17] Manekar M A, Chaudhary S, Chattopadhyay M K, Singh K J, Roy S B and Chaddah P 2001 *Phys. Rev.* B **64** 104416
Chattopadhyay M K, Roy S B and Chaddah P 2005 *Phys. Rev.* B **72** 180401(R)

[18] Banerjee A, Mukherjee K, Kumar K and Chaddah P 2006 *Phys. Rev.* B **74** 224445
[19] Banerjee A, Pramanik A K, Kumar K and Chaddah P 2006 *J. Phys.: Condens. Matter* **18** L605
[20] Singh K J, Chaudhary S, Chattopadhyay M K, Manekar M A, Roy S B and Chaddah P 2002 *Phys. Rev.* B **65** 094419
[21] Roy S B, Chattopadhyay M K, Chaddah P, Moore J D, Perkins G K, Cohen L F, Gschneidner K A Jr and Pecharsky V K 2006 *Phys. Rev.* B **74** 012403
[22] Sengupta K and Sampathkumaran E V 2006 *Phys. Rev.* B **73** 020406
[23] Chaddah P, Banerjee A and Roy S B 2006 *Preprint* cond-mat/0601095v1
[24] Hernandez-Minguez A, Macia F, Hernandez J M, Abril G, Garcia-Santiago A, Tejada J and Parisi F 2007 *Preprint* cond-mat/0705.1257v1
[25] Imry Y and Wortis M 1979 *Phys. Rev.* B **19** 3580
[26] Baranov N V and Baranova E A 1995 *J. Alloys Compounds* **219** 139
[27] Kumar K, Pramanik A K, Banerjee A, Chaddah P, Roy S B, Park S, Zhang C L and Cheong S-W 2006 *Phys. Rev.* B **73** 184435
[28] Chaddah P 2006 *Pramana J. Phys.* **67** 113
[29] Roy S B, Chattopadhyay M K, Banerjee A, Chaddah P, Moore J D, Perkins G K, Cohen L F, Gschneidner K A Jr and Pecharsky V K 2007 *Phys. Rev.* B **75** 184410